AGU ADVANCING EARTH AND SPACE SCIENCE

Water Resources Research

RESEARCH ARTICLE
10.1029/2020WR028539

A Simple Correction Term to Model Infiltration in Water-Repellent Soils

M. R. Abou Najm[1,2], Ryan D. Stewart[3], Simone Di Prima[4,5], and Laurent Lassabatere[5]

[1]Department of Land, Air and Water Resources, University of California, Davis, CA, USA, [2]John Muir Institute of the Environment, University of California, Davis, CA, USA, [3]School of Plant and Environmental Sciences, Virginia Polytechnic Institute and State University, Blacksburg, VA, USA, [4]Department of Agricultural Sciences, University of Sassari, Sassari, Italy, [5]UMR5023 Ecologie des Hydrosystèmes Naturels et Anthropisés, CNRS, ENTPE, Université de Lyon 1, Bouguenais, France

Key Points:

- We propose a simple correction term for infiltration models to characterize water repellency in infiltration models
- One hundred and sixty five infiltration experiments from three different ecosystems and levels of water repellencies were used to demonstrate model effectiveness
- The one parameter correction substantially reduced model error and reflected the changing rate of water repellency during infiltration

Supporting Information:

- Data Set S1

Correspondence to:
M. R. Abou Najm,
mabounajm@ucdavis.edu

Citation:
Abou Najm, M. R., Stewart, R. D., Di Prima, S., & Lassabatere, L. (2021). A simple correction term to model infiltration in water-repellent soils. *Water Resources Research*, *57*, e2020WR028539. https://doi.org/10.1029/2020WR028539

Received 10 AUG 2020
Accepted 12 JAN 2021

Abstract Soil water repellency can substantially alter hydrologic processes, particularly the ability of soils to infiltrate water. Water repellency often changes through time, making it difficult to simulate infiltration behaviors of water-repellent soils using standard models. Here, we propose a simple rate-based correction term that starts with a value of zero at the beginning of the infiltration process ($t = 0$) and asymptotically approaches 1 as time increases, thus simulating decreasing soil water repellency through time. The correction term can be used with any infiltration model. For this study, we selected a simple two-term infiltration equation and then, using two data sets of infiltration measurements conducted in soils with varying water repellency, compared model error with versus without the added term. The correction substantially reduced model error, particularly in more repellent soils. At the same time, the rate constant parameter introduced in the new model may be useful to better understand dynamics of soil water repellency and to provide more consistent interpretations of hydraulic properties in water-repellent soils.

1. Introduction

Water repellency can form in soils under a wide spectrum of conditions, including deposition of resinous materials and exudates from vegetation (Lichner et al., 2018), vaporization and condensation of organic compounds during fires (DeBano et al., 1970), and presence of anthropogenic-derived chemicals such as petroleum products (Adams et al., 2008; Badin et al., 2008; Hewelke et al., 2018; Roy & McGill, 2000), wastewater (Arye et al., 2011) or other urban contaminants (Stavi & Rosenzweig, 2020). Soil water repellency can range from mild to severe, with the latter often considered to represent hydrophobic conditions. When present, soil water repellency affects many aspects of the hydrological cycle, including infiltration, surface runoff, and evaporation (Bauters et al., 2000; Doerr et al., 2006; Ebel et al., 2012; Imeson et al., 1992; Mansell, 1970; Rye & Smettem, 2017). These effects can extend to watershed-scale responses, such as increased flooding and debris flows (Ebel et al., 2016; McGuire et al., 2018; Rengers et al., 2019).

Soil water repellency often diminishes or dissipates in the presence of liquid water (Dekker et al., 2001; Doerr & Thomas, 2000), meaning that infiltration can reduce water repellency through time. This interaction in turn often causes infiltration rates to gradually increase (J. Chen, Pangle, et al., 2020; Ebel et al., 2016; Robichaud, 2000). This dynamic process results in atypical infiltration behaviors, for example, cumulative infiltration forming upwardly convex curves with time (Concialdi et al., 2020; Di Prima et al., 2017; Li et al., 2018). However, many studies continue to use standard equations, such as the two-term model first developed by Philip (1957), to simulate infiltration in fire-affected and other water-repellent soils (Ebel & Moody, 2020; McGuire et al., 2018; Moody et al., 2019). This approach can require extensive calibration (L. Chen, Berli, et al., 2013), which often results in nonphysical parameters, for example, negative or null values for hydraulic conductivity (Di Prima et al., 2019).

Here, we propose a simple correction term $\left(1 - e^{-\alpha_{WR} t}\right)$ to modify models for infiltration rate. The correction term starts with a value of zero at the beginning of the infiltration experiment ($t = 0$) and asymptotically approaches 1 as time increases, thus simulating decreasing soil water repellency through time. Furthermore,

the correction only uses a single rate-constant parameter (α_{WR}), whose reciprocal reflects the time-scale of water repellency, and thus may be useful to characterize the duration of water repellency.

1.1. Theory

Water repellency often delays the start of infiltration and attenuates infiltration rates, particularly at the early times of rainfall or irrigation events. We model this response using an exponential scaling factor:

$$i_{WR}(t) = i(t)\left(1 - e^{-\alpha_{WR} t}\right) \tag{1}$$

where $i_{WR}(t)$ is the scaled infiltration rate [LT^{-1}], $i(t)$ is the unscaled infiltration rate (i.e., as modeled using a wide range of conventional equations of infiltration models that do not account for water repellency) [LT^{-1}], t is the time elapsed since the start of the infiltration event [T], and α_{WR} is a newly introduced empirical soil parameter [T^{-1}] that describes the rate of attenuation of infiltration rate. α_{WR} can be considered to be a rate constant associated with change in water repellency through time. Here, we stress that Equation 1 is broadly defined and can be used with any infiltration model (short-term, steady state, one-dimensional, two-dimensional, or three-dimensional). The correction factor can quantify the effect of water repellency at the soil surface without impacting the physical models used, so that $i(t)$ continues to be quantified using common soil hydraulic properties (e.g., soil sorptivity and hydraulic conductivity). Such correction typically applies to fire-induced water repellency or factors that affect the soil mainly at surface (vegetation inputs).

We can also define a characteristic time for water repellency, t_{WR} [T], as:

$$t_{WR} = \ln(2) / \alpha_{WR} \tag{2}$$

Based on Equation 2, t_{WR} represents the time at which the infiltration rate of the water-repellent soil is half that of the equivalent nonrepellent soil, that is, $i_{WR}(t)/i(t) = 0.5$. In other words, t_{WR} identifies the time at which the term $\left(1 - e^{-\alpha_{WR} t}\right) = 0.5$. We will use this concept to test the hypothesis that infiltration rates are affected for longer periods of time in soils with more severe water repellency.

To demonstrate the effectiveness of this method, we use a simple two-term infiltration model (Stewart & Abou Najm, 2018a; Vandervaere et al., 2020a, 2020b):

$$I(t) = c_1 t^{1/2} + c_2\, t \tag{3}$$

where c_1 [$LT^{-1/2}$] and c_2 [$L\ T^{-1}$] are constants specific to the soil type and initial and boundary conditions (e.g., ponding depth, ring geometry, initial water content). For example, in the one-dimensional, Philip (1969) model for vertical infiltration, c_1 is sorptivity (S) [$LT^{-1/2}$] and c_2 is A [$L\ T^{-1}$] (a term related to hydraulic conductivity).

The infiltration rate, i [$L\ T^{-1}$], for the two-term model of Equation 3 is

$$i(t) = \frac{c_1}{2\sqrt{t}} + c_2 \tag{4}$$

Here we modify Equation 4 to account for water repellency, $i_{WR}(t)$ [$L\ T^{-1}$], as:

$$i_{WR}(t) = i(t)\left(1 - e^{-\alpha_{WR} t}\right) = \left(\frac{c_1}{2\sqrt{t}} + c_2\right)\left(1 - e^{-\alpha_{WR} t}\right) \tag{5}$$

Cumulative infiltration, I_{WR} [L], is then found by integrating Equation 5 with respect to time:

$$I_{WR}(t) = c_1\sqrt{t} - \frac{c_1\sqrt{\pi}}{2\sqrt{\alpha_{WR}}} erf\left(\sqrt{\alpha_{WR} t}\right) + c_2 t - \frac{c_2\left(1 - e^{-\alpha_{WR} t}\right)}{\alpha_{WR}} \tag{6}$$

Equation 6 can be written as:

$$I_{WR}(t) = c_1\sqrt{t} - \frac{c_1\sqrt{\pi}}{2\sqrt{\alpha_{WR}}}(1 - \frac{e^{-\alpha_{WR}t}}{\sqrt{\pi\alpha_{WR}t}}g(t)) + c_2 t - \frac{c_2\left(1 - e^{-\alpha_{WR}t}\right)}{\alpha_{WR}} \quad (7)$$

where $g(t)$ is approximated as (Winitzki, 2003):

$$g(t) \approx \frac{\sqrt{\pi\alpha_{WR}t} + (\pi - 2)\alpha_{WR}t}{1 + \sqrt{\pi\alpha_{WR}t} + (\pi - 2)\alpha_{WR}t} \quad (8)$$

Combining Equations 7 and 8:

$$I_{WR}(t) \approx c_1\sqrt{t} + c_2 t - \frac{c_1\sqrt{\pi}}{2\sqrt{\alpha_{WR}}}\left(1 - e^{-\alpha_{WR}t}\left(\frac{1 + \sqrt{\pi\alpha_{WR}t} - 2\sqrt{\alpha_{WR}t/\pi}}{1 + \sqrt{\pi\alpha_{WR}t} + (\pi - 2)\alpha_{WR}t}\right)\right) - \frac{c_2\left(1 - e^{-\alpha_{WR}t}\right)}{\alpha_{WR}} \quad (9)$$

Figure 1 shows typical infiltration rates and cumulative infiltration curves of a silty clay loam soil (Di Prima, Winiarski, et al., 2020) and how the shapes of the curves change with different α_{WR} values. Clearly, the infiltration rates become attenuated as α_{WR} values decrease, reflecting increased effect of soil water repellency. The model also shows an increase followed by decrease of infiltration rate for many α_{WR} values, which reflects common observations of infiltration in water repellent soils (e.g., J. Chen, McGuire, et al., 2020; Imeson et al., 1992).

2. Materials and Methods

We analyzed two data sets to test our model: one was collected following wildfires that occurred in the south-central Appalachian Mountains, USA, and the other was collected in four locations in Spain and France and assessed water repellency due to different inputs and in particular vegetation and fire effects.

2.1. Wildfire Study

Data from 150 repeated tension infiltrometer experiments were used to assess the ability of α_{WR} to model the effect of hydrophobicity. The infiltration measurements were collected in burned versus unburned sites in Mount Pleasant National Wildlife Refuge, Virginia, USA (37.73, −79.21), which experienced moderate to severe wildfires in November 2016. Here, we will refer to the sites as Burned 1 (41 experiments), Burned 2 (41 experiments), Unburned 1 (35 experiments), and Unburned 2 (33 experiments). The sites (Site 1 and Site 2) were on west-facing back slopes and shoulders. Within each site, infiltration tests occurred with spacing of 1–2 m between measurements. For each test, a mini-disk tension infiltrometer (Meter Group, Pullman, Washington, USA) was used with tension set to −1 cm. This tension was selected to ensure water flow occurred through all pores <0.3 cm in diameter (based on the Youngs-Laplace equation) while avoiding potential measurement errors associated with water entry into larger dead-end pores. Water volumes were recorded every 0.5 min, and continued for a minimum of 10 readings. Measurements were collected on the following dates: November 28, 2016 (3 days after fire); February 6, 2017 (73 days after fire); March 24, 2017 (116 days after fire); May 18, 2017 (171 days after fire); June 27, 2017 (211 days after fire); August 22, 2017 (267 days after fire); October 3, 2017 (309 days after fire); and December 4, 2017 (371 days after fire).

Soil water repellency was measured at the same times and general locations as the infiltration tests. Here, water drop penetration time (WDPT) tests were conducted using an eye dropper. The soil or ash layer surface was cleared of any loose debris, and 5–7 drops were placed on the surface (0 cm depth). The time for the drops to infiltration was noted, with tests divided into two categories: WDPT <10 s versus WDPT ≥10 s (J. Chen, McGuire, et al., 2020). The test was repeated at 10 discrete locations within each sampling area. Water repellency was then quantified as the percentage of drops with WDPT ≥ 10 s over the total number

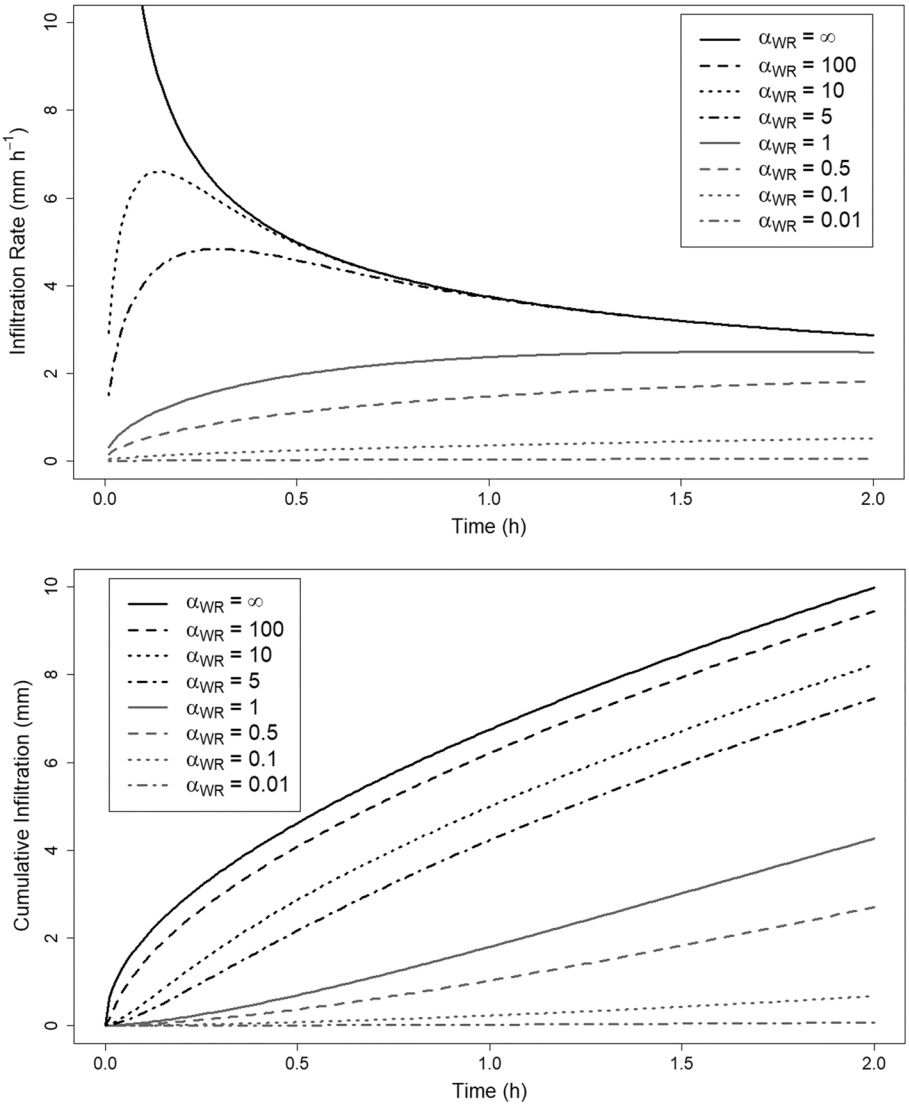

Figure 1. Ideal infiltration rate (upper panel) and cumulative infiltration (lower panel) curves (dark full line) of a silty clay loam soil ($S = 6$ mm h$^{-1/2}$, 10% saturation, $A = 0.75$ mm h^{-1}) respectively modeled by Equations 5 and 6 using data from Di Prima, et al. (2020) and synthetic variations of possible hydrophobic responses demonstrated by a range of α_{WR} values from 0.01 to 100 h^{-1}.

of tests at a given sampling point. For more details, the reader is referred to J. Chen, McGuire, et al. (2020) and J. Chen, Pangle, et al. (2020).

The three parameters (c_1, c_2, and α_{WR}) were optimized for each infiltration test by minimizing the sum of square of errors (SSE) between measured and modeled cumulative infiltration. Note that we choose to fit cumulative infiltration (using Equation 9) rather than infiltration rate because the former was better constrained at early times (with $I = 0$ at $t = 0$) and the measured cumulative infiltration data had less noise than the infiltration rate data.

All 150 experiments were optimized with 41 sets of initial parameter values for c_1, c_2, and α_{WR}, using all permutations of the following quantities: $c_1 = 0.001$, 0.01, 0.1, 1, and 10 cm min$^{-1/2}$; $c_2 = 0.001$, 0.01, 0.1, 1, and 10 cm min^{-1}, and $\alpha_{WR} = 0.001$, 0.01, 0.1, 1, and 10 min^{-1}. The parameter set with the smallest SSE was chosen as the global optimum solution. Cumulative histograms were developed for the optimized parameters (c_1, c_2, and α_{WR}) under each of the four groups: Burned 1 ($N = 41$), Burned 2 ($N = 41$), Unburned 1 ($N = 35$),

and Unburned 2 ($N = 33$). The α_{WR} values were also converted to t_{WR} using Equation 2, and the mean t_{WR} for each site and sampling date was compared to the corresponding water repellency.

For comparison, we also analyzed the data using the two-term infiltration solution (Equation 3), in this case optimizing for only c_1 and c_2. The same initial parameter values were used for c_1 and c_2, and again the global optimum set of values was identified for each test. The sum of square errors (SSE) from Equation 3 ($SSE_{no\,\alpha}$) was then compared with SSE from Equation 9 (SSE_{α}).

We also evaluated if the parameter distributions varied between sites. Since all three parameters (c_1, c_2, and α_{WR}) were nonnormally distributed, even after log-transformation, we performed one-way Kruskal-Wallis tests for each parameter using site as the main factor. For any parameter with significant differences between sites, we performed a posthoc Dunn test with the Benjamini-Hochberg method for p-value adjustments. We used a significance level (alpha) of 0.05. Statistical analyses were conducted using *R* (version 4.0.3).

2.2. Vegetation-Induced Repellency Study

Fifteen infiltration experiments from three locations in Spain and France were also used to assess the effectiveness of Equation 9 compared to Equation 3. Those experiments were divided as follows: eight experiments from La Hunde site in Spain (Di Prima et al., 2017); five experiments from two locations in Django infiltration basin, France (Di Prima, Winiarski, et al., 2020 and unpublished data); and two experiments from ENTPE garden, in France (Concialdi et al., 2020). The infiltration tests were conducted using single ring infiltrometers with inner ring diameter of 15 cm. For each test, the rings were inserted into the soil at a depth of ~1 cm. Slightly ponded conditions were maintained in the rings and the rate of water additions to the rings were recorded to determine infiltration rates. Soil physical properties of those sites spanned a wide spectrum of textural classes, as briefly described below.

The La Hunde site in Valencia, Spain (Di Prima et al., 2017) consisted of two contiguous plots, each of 1800 m^2, located at the headwaters of Rambla Espadilla catchment within the public forest La Hunde (39°4'50"N, 1°14'47"W, elevation of 1,090 m a.s.l.), Valencia (NE Spain). Plots were located in a typical Mediterranean oak forest approximately 60 years old, characterized by *Quercus ilex* sbsp. *Ballota* in association with other xerophytic species such as *Pinus halepensis*, *Quercus faginea*, *Juniperus phoenicea*, and *Juniperus oxycedrus*. The climate was Mediterranean with a mean annual rainfall of 466 mm and a mean annual temperature of 13.7°C (1960–2007). According to the USDA standards, the soil of the studied area was classified as clay loam. The soil was approximately 30–50 cm deep in the lower part of the slope and about 10 cm thick in higher elevations, with rock fragments constituting up to 50% of the soil volume (del Campo et al., 2019).

The Django site occurred within a stormwater infiltration basin, named Django Reinhardt basin, located in Chassieu in the eastern suburbs of Lyon, France (Di Prima, Winiarski, et al., 2020). A detailed description of the experimental area can be found in Goutaland et al. (2008) and Winiarski et al. (2006). The infiltration basin was constructed above a heterogeneous glaciofluvial deposit by mixing the top 50–80 cm of the soil. The coarse glaciofluvial deposit was composed of four main lithofacies: (i) the upper sandy layer that was a mixture of the soil matrix and gravel, (ii) a mixture of the soil matrix and gravel with a bimodal particle size distribution that occupied most of the deposit below the top 50–80 cm layer, (iii) large lenses of sand, and (iv) smaller lenses of matrix-free gravel (Ben Slimene et al., 2017; Goutaland et al., 2013). At surface, a sedimentary layer was deposited with high contents of organic matter, impeding water infiltration at the basin scale (Lassabatere et al., 2010). The high organic contents resulted from both vegetation and pollutants loads brought by the entering stormwater (Badin et al., 2008).

The ENTPE site in Lyon, France (Concialdi et al., 2020) contained a sandy loam soil located in the garden of the École Nationale des Travaux Publics de l'État (ENTPE) in the municipality of Vaulx-en-Velin (France). The site was chosen to represent a typical rain garden developed to restore hydrological processes (i.e., water infiltration capacity) in urban areas.

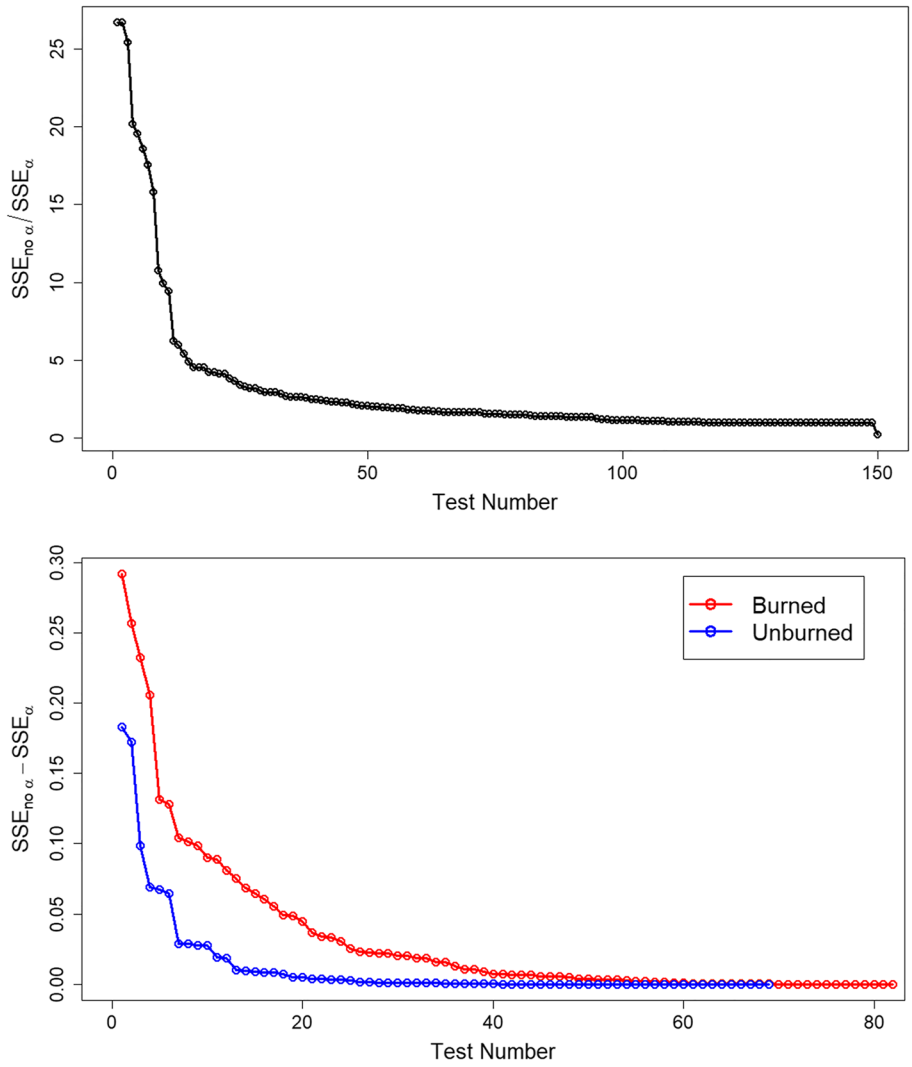

Figure 2. Upper panel shows ratios of SSE values ($SSE_{no\ \alpha}/SSE_{\alpha}$) and lower panel shows differences ($SSE_{no\alpha}$–SSE_{α}) between Equation 3 (no α_{WR}) and Equation [9] (with α_{WR}) for the 150 infiltration experiments from two burned and unburned areas. Note that the runs are organized in decreasing order in each panel.

3. Results and Discussion

3.1. Wildfire Induced Water Repellency

The proposed model (Equation 1, approximated for the two-parameter model by Equation 9) provided better fits to measured data compared to the standard infiltration model (Equation 3) for most of the measurements (Figure 2). Specifically, the ratio of $SSE_{no\ \alpha}/SSE_{\alpha}$ was greater than 1 for 116 out of 150 infiltration tests, and was less than 1 for only 2 out of 150 infiltration tests (Figure 2a). Equation 9 improved the model fit more in burned compared to unburned soils, as difference in SSE between Equation 3 ($SSE_{no\ \alpha}$) versus Equation 9 (SSE_{α}) was larger for the former (Figure 2b).

The cumulative histograms of parameter values for the wildfire study (Figure 3) showed that both burned areas (Burned 1 and Burned 2) had smaller median α_{WR} values than the unburned areas (Unburned 1 and Unburned 2). The Kruskal-Wallis test indicated that α_{WR} distributions were significantly different between sites ($p = 0.0011$), and the posthoc Dunn test revealed that the Burned 2 site had significantly smaller α_{WR} values than the other three sites ($0.003 < p < 0.028$). That site experienced the greatest burn severity (J. Chen, McGuire, et al., 2020) and in general had the strongest water repellency at the surface (J. Chen, Pangle, et al., 2020). Since smaller values of α_{WR} correspond to longer-lasting water repellency (as shown in

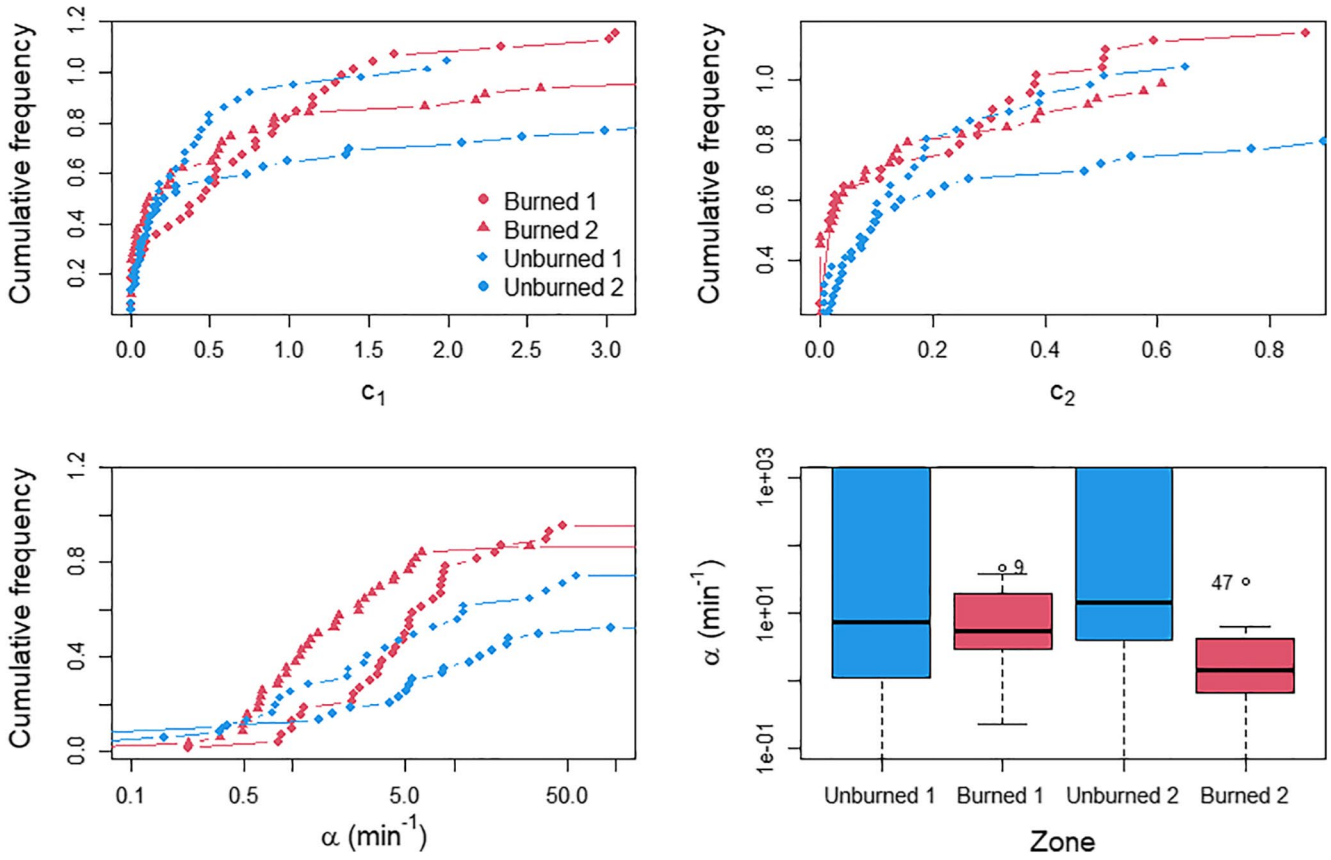

Figure 3. Cumulative histogram for α_{WR} (min^{-1}), c_1 (cm $min^{-1/2}$), and c_2 (cm min^{-1}) for the 150 infiltration experiments from two burned and unburned areas, box plot of the distributions for α_{WR} (min^{-1}) for the four zones (sites 1 and 2, burned and unburned zones).

Figure 1), this result indicates that the α_{WR} parameter successfully adjusted the infiltration model to fit to hydrophobic conditions.

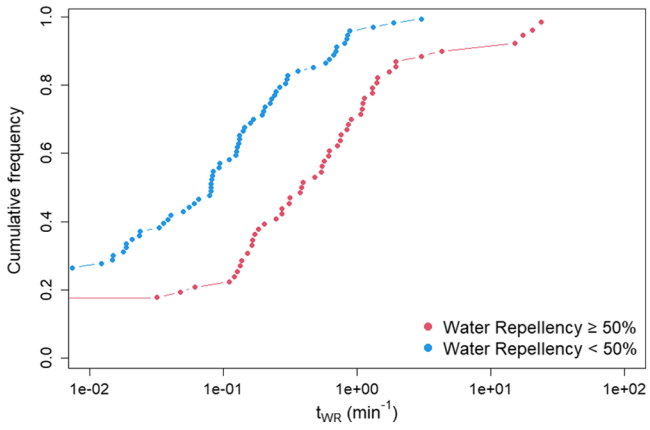

Figure 4. Cumulative frequency distributions for characteristic water repellency time, t_{WR} (min), for infiltration measurements collected when the surface soils exhibited low (≤50%) or high (>50%) water repellency, as assessed using multiple water drop penetration time tests. Vegetation-induced water repellency.

Furthermore, Figure 3 also shows that the c_1 and c_2 parameters did not show substantial differences in their distributions between burned and unburned sites, Those results were further supported by the Kruskal-Wallis tests, which determined that c_1 and c_2 did not significantly differ between sites ($p > 0.05$). Taken together, these findings suggest the fires may not have induced permanent changes in soil hydraulic properties (e.g., sorptivity and hydraulic conductivity), and moreover that the proposed scaling factor can account for transient changes to those properties due to soil water repellency. Nonetheless, additional tests, such as laboratory characterization, would be necessary to fully support or refute this hypothesis.

We also separated the infiltration measurements based on the relative water repellency measured on each sampling date. Specifically, measurements were grouped into those that occurred when 50% or more of the WDPT tests were less than 10 s (i.e., water repellency ≤50%) and those that occurred when the majority of WDPT tests exceeded 10 s (i.e., water repellency >50%). The t_{WR} values were consistently higher for tests conducted when the soil was more water-repellent (Figure 4). For example, t_{WR} was greater than 0.1 min for about 80% of tests conducted when water repellency exceeded 50%, whereas only about 40% of tests under low water repellency had t_{WR} values greater than 0.1 min. These results imply

Table 1
Results From 15 Infiltration Experiments Demonstrating the Effectiveness of Proposed Exponential Scaling Factor $(1-e^{-\alpha_{WR}t})$ *by Comparing Equation 3 With Equation 9*

Site	Reference	Run	Equation 3			Equation 9				$SSE_{no\alpha}/SSE_{\alpha}$
			c_1	c_2	$SSE_{no\alpha}$	c_1	c_2	α_{WR}	SSE_{α}	
La Hunde (Spain)	Di Prima et al. (2017)	5	0.00	0.19	836	5.79	0.10	0.006	170	4.89
		14	0.00	0.14	640	5.45	0.07	0.004	192	3.33
		2	0.00	0.24	721	7.17	0.13	0.006	41	17.76
		16	0.00	0.26	459	0.00	0.30	0.027	61	7.44
		13	0.00	0.09	780	4.86	0.05	0.002	123	6.32
		18	1.19	0.33	45	1.19	0.33	>100	45	1.00
		1	0.00	0.41	1,515	11.82	0.30	0.007	31	48.31
		11	0.00	0.19	549	0.00	0.22	0.020	61	8.96
Django (France)	Di Prima et al. (2020b)	34	0.00	0.24	13,404	10.08	0.14	0.003	1,036	130.09
		10	0.00	0.14	53,264	9.45	0.17	0.001	681	78.16
		40	0.00	0.21	56,274	7.43	0.35	0.001	159	353.23
		75	0.00	0.13	1962	6.18	0.12	0.002	33	59.34
		76	0.00	0.28	1,514	9.42	0.12	0.005	58	26.02
ENTPE-1 (France)	Concialdi et al. (2020)	4	0.00	0.02	938	0.00	0.02	0.005	270	3.47
		8	0.00	0.03	3,465	0.00	0.03	0.003	431	8.03

that the magnitude of t_{WR} may be related to soil water repellency, providing some support to our initial hypothesis. However, future studies should explore this relationship more carefully, for example by measuring water repellency in direct conjunction with infiltration (Tillman et al., 1989).

In the study of vegetation-induced repellency, Equation 9 gave better fits to observations (i.e., $SSE_{no\,\alpha}/SSE_{\alpha} > 1$) for 14 out of 15 infiltration experiments (Table 1 and Figure 5). The remaining site showed no change (i.e., $SSE_{no\,\alpha}/SSE_{\alpha} = 1$), possibly due to limited effect of water repellency in those instances. Using Equation 9 also resulted in the c_1 parameter being >0 for all but four infiltration experiments. In contrast, $c_1 = 0$ was obtained for 14 out of 15 infiltration tests when the uncorrected Equation 3 was used. Since c_1 is often considered to represent soil sorptivity (Stewart & Abou Najm, 2018a, 2018b), values of 0 are only physically plausible in saturated conditions. Future studies should consider whether the use of Equation 9 can be used to accurately constrain hydraulic parameters such as sorptivity and hydraulic conductivity from infiltration tests conducted in water-repellent soils.

The need for new approaches to deal with infiltration into water-repellent soils has been discussed in previous studies. For instance, the BEST methods that were used for the characterization of soil water retention and hydraulic conductivity functions currently only apply to concave curves (Angulo-Jaramillo et al., 2019), and not the convex curves typical of water-repellent soils. With our model, and its time-dependent water repellency term $\left(1-e^{-\alpha_{WR}t}\right)$, we can now deduce unscaled cumulative infiltration (i.e., infiltration driven by capillarity and gravity without water repellency) from Equation 1:

$$i(t) = \frac{i_{WR}(t)}{\left(1-e^{-\alpha_{WR}t}\right)} \tag{10}$$

The integration of the corrected infiltration rate $i(t)$ will provide the corresponding corrected cumulative infiltration rate. Using this approach may make it possible to use BEST or other algorithms and derive soil hydraulic parameters from convex cumulative infiltration curves. At the same time, the relative consistency of hydraulic parameters c_1 and c_2 identified in the wildfire study (Figure 3) suggests that this approach may assist in a complete characterization of hydrophobic soils. We note, however, that additional measurements

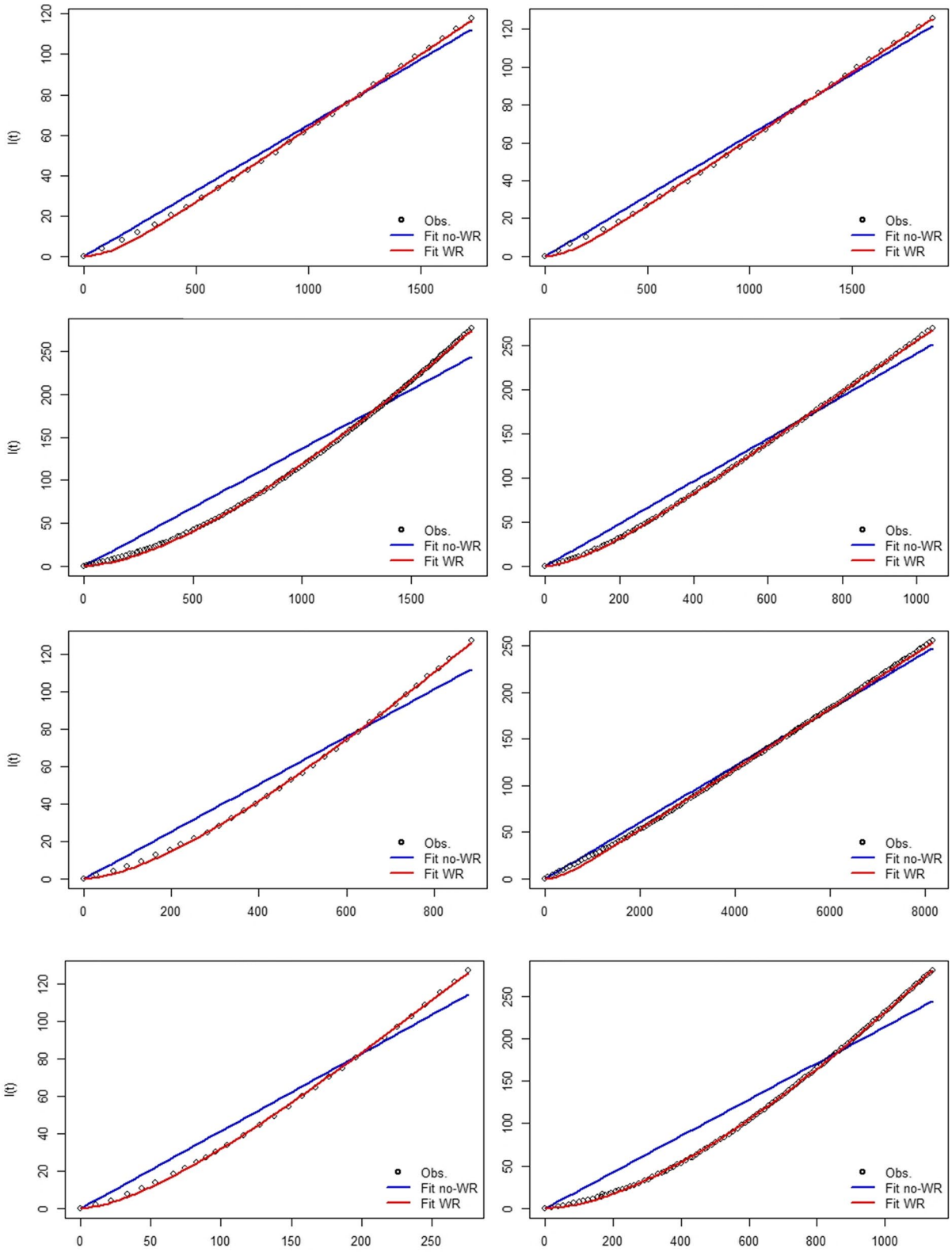

Figure 5. Examples from each of the three locations comparing experimental results from infiltration experiments (circles) to results from Equation 3 (blue) and Equation 9 (red).

(e.g., WDPTs) may still be required, particularly since models modified with the correction term may suffer from equifinality or related sources of uncertainty when fit solely to infiltration data (Beven, 2006). This topic should be the subject of further research.

4. Conclusion

An exponential scaling factor $\left(1 - e^{-\alpha_{WR} t}\right)$ was proposed to model the effect of water repellency and hydrophobicity in infiltration models. The model contains one additional parameter (α_{WR}), which can be considered to reflect the rate at which water repellency diminishes during infiltration. Though empirical in nature, α_{WR} can be used to derive a characteristic time, t_{WR}, at which infiltration rates recover to some percentage (e.g., 50%) of infiltration under nonrepellent conditions. The time t_{WR} may be considered as a characteristic time for water repellency, and therefore may be comparable with other types of characteristics times such as water drop penetration test (WDPT) times.

Results for 165 infiltration experiments—representing different ecosystems with a variety of sources and levels of soils water repellency—were used to demonstrate the effectiveness of this simple method to characterize water repellency in infiltration models. For example, the analysis showed that α_{WR} has smaller values in soils that were burned during a wildfire compared to unburned controls. The magnitude of t_{WR} also had some correlation with the amount of water repellency measured at the time of infiltration, suggesting that it may be useful as a way to characterize the degree and persistence of soil water repellency.

Even though we focused our comparisons on variations of a widely used two-term infiltration equation, the scaling factor can be applied to any infiltration model. In addition, the proposed approach could be combined with other approaches to offer the complete determination of soil hydraulic properties, including hydrophobicity. Future work may therefore consider questions such as whether the α parameter can be predicted based on other indicators (e.g., WDPT times) and if it can provide a consistent measure for both the degree and duration of water repellency.

Data Availability Statement

Dr. Jingjing Chen led the field measurements for the wildfire study. Data are available through J. Chen, McGuire, et al. (2020), J. Chen, Pangle, et al. (2020), Di Prima et al., (2017), Di Prima, Stewart, et al. (2020), and Concialdi et al., (2020) and are summarized in a zip file containing all.csv and. r files used in the Supplement Files (WRR_Infiltration_correction_Data.zip). Data are also available and will be permanently archived at https://data.lib.vt.edu/files/3197xm23r.

Acknowledgments
The authors would like to acknowledge the helpful suggestions from Professor Teamrat Ghezzehei, who suggested to consider applying the scaling factor to the infiltration rate instead of cumulative infiltration. Funding for this work was provided in part by the University of California–Davis, Agricultural Experiment Station, the Virginia Agricultural Experiment Station and the Multistate Hatch Program W4188 of the USDA, National Institute of Food and Agriculture. This work was also supported through the INFILTRON Project (ANR--17-CE04-0010, Package for assessing infiltration & filtration functions of urban soils in stormwater management; https://infiltron.org/) funded by the French National Research Agency (ANR).

References

Adams, R. H., Guzmán Osorio, F. J., & Zavala Cruz, J. (2008). Water repellency in oil contaminated sandy and clayey soils. *International journal of Environmental Science and Technology*, *5*(4), 445–454. https://doi.org/10.1007/BF03326040

Angulo-Jaramillo, R., Bagarello, V., Di Prima, S., Gosset, A., Iovino, M., & Lassabatere, L. (2019). Beerkan Estimation of Soil Transfer parameters (BEST) across soils and scales. *Journal of Hydrology*, *576*, 239–261. https://doi.org/10.1016/j.jhydrol.2019.06.007

Arye, G., Tarchitzky, J., & Chen, Y. (2011). Treated wastewater effects on water repellency and soil hydraulic properties of soil aquifer treatment infiltration basins. *Journal of Hydrology*, *397*(1–2), 136–145. https://doi.org/10.1016/j.jhydrol.2010.11.046

Badin, A.-L., Faure, P., Bedell, J.-P., & Delolme, C. (2008). Distribution of organic pollutants and natural organic matter in urban storm water sediments as a function of grain size. *The Science of the Total Environment*, *403*(1–3), 178–187. https://doi.org/10.1016/j.scitotenv.2008.05.022

Bauters, T. W. J., Steenhuis, T. S., DiCarlo, D. A., Nieber, J. L., Dekker, L. W., Ritsema, C. J., et al. (2000). Physics of water repellent soils. *Journal of Hydrology*, *231–232*, 233–243. https://doi.org/10.1016/S0022-1694(00)00197-9

Ben Slimene, E., Lassabatere, L., Šimůnek, J., Winiarski, T., & Gourdon, R. (2017). The role of heterogeneous lithology in a glaciofluvial deposit on unsaturated preferential flow: A numerical study. *Journal of Hydrology and Hydromechanics*, *65*(3), 209–221. https://doi.org/10.1515/johh-2017-0004

Beven, K. (2006). A manifesto for the equifinality thesis. *Journal of Hydrology*, *320*(1–2), 18–36. https://doi.org/10.1016/j.jhydrol.2005.07.007

Chen, L., Berli, M., & Chief, K. (2013). Examining modeling approaches for the rainfall-runoff process in Wildfire-affected watersheds: Using San Dimas experimental forest. *JAWRA Journal of the American Water Resources Association*, *49*(4), 851–866. https://doi.org/10.1111/jawr.12043

Chen, J., McGuire, K. J., & Stewart, R. D. (2020). Effect of soil water-repellent layer depth on post-wildfire hydrological processes. *Hydrological Processes*, *34*(2), 270–283. https://doi.org/10.1002/hyp.13583

Chen, J., Pangle, L. A., Gannon, J. P., & Stewart, R. D. (2020). Soil water repellency after wildfires in the Blue Ridge Mountains. *International Journal of Wildland Fire*, *29*(11), 1009–1020. Retrieved from https://www.publish.csiro.au/WF/WF20055. https://doi.org/10.1071/WF20055; https://doi.org/10.3390/su13010227

Concialdi, P., Di Prima, S., Bhanderi, H. M., Stewart, R. D., Abou Najm, M. R., Lal Gaur, M., et al. (2020). An open-source instrumentation package for intensive soil hydraulic characterization. *Journal of Hydrology*, *582*, 124492. https://doi.org/10.1016/j.jhydrol.2019.124492

DeBano, L. F., Mann, L. D., & Hamilton, D. A. (1970). Translocation of hydrophobic substances into soil by burning organic litter. *Soil Science Society of America Journal*, *34*(1), 130–133. https://doi.org/10.2136/sssaj1970.03615995003400010035x

Dekker, L. W., Doerr, S. H., Oostindie, K., Ziogas, A. K., & Ritsema, C. J. (2001). Water repellency and critical soil water content in a dune sand. *Soil Science Society of America Journal*, *65*(6), 1667. https://doi.org/10.2136/sssaj2001.1667

del Campo, A. D., González-Sanchis, M., García-Prats, A., Ceacero, C. J., & Lull, C. (2019). The impact of adaptive forest management on water fluxes and growth dynamics in a water-limited low-biomass oak coppice. *Agricultural and Forest Meteorology*, *264*, 266–282. https://doi.org/10.1016/j.agrformet.2018.10.016

Di Prima, S., Bagarello, V., Angulo-Jaramillo, R., Bautista, I., Cerdà, A., del Campo, A., et al. (2017). Impacts of thinning of a Mediterranean oak forest on soil properties influencing water infiltration. *Journal of Hydrology and Hydromechanics*, *65*(3), 276–286. https://doi.org/10.1515/johh-2017-0016

Di Prima, S., Castellini, M., Abou Najm, M. R., Stewart, R. D., Angulo-Jaramillo, R., Winiarski, T., et al. (2019). Experimental assessment of a new comprehensive model for single ring infiltration data. *Journal of Hydrology*, *573*, 937–951. https://doi.org/10.1016/j.jhydrol.2019.03.077

Di Prima, S., Stewart, R. D., Castellini, M., Bagarello, V., Abou Najm, M. R., Pirastru, M., et al. (2020). Estimating the macroscopic capillary length from Beerkan infiltration experiments and its impact on saturated soil hydraulic conductivity predictions. *Journal of Hydrology*, *589*, 125159. https://doi.org/10.1016/j.jhydrol.2020.125159

Di Prima, S., Winiarski, T., Angulo-Jaramillo, R., Stewart, R. D., Castellini, M., Abou Najm, M. R., et al. (2020). *Detecting infiltrated water and preferential flow pathways through time-lapse ground-penetrating radar surveys*. (pp. 138511). Science of The Total Environment. https://doi.org/10.1016/j.scitotenv.2020.138511

Doerr, S. H., Shakesby, R. A., Blake, W. H., Chafer, C. J., Humphreys, G. S., & Wallbrink, P. J. (2006). Effects of differing wildfire severities on soil wettability and implications for hydrological response. *Journal of Hydrology*, *319*(1), 295–311. https://doi.org/10.1016/j.jhydrol.2005.06.038

Doerr, S. H., & Thomas, A. D. (2000). The role of soil moisture in controlling water repellency: new evidence from forest soils in Portugal. *Journal of Hydrology*, *231–232*, 134–147. https://doi.org/10.1016/S0022-1694(00)00190-6

Ebel, B. A., & Moody, J. A. (2020). Parameter estimation for multiple post-wildfire hydrologic models. *Hydrological Processes*, *34*, 4049–4066. https://doi.org/10.1002/hyp.13865

Ebel, B. A., Moody, J. A., & Martin, D. A. (2012). Hydrologic conditions controlling runoff generation immediately after wildfire. *Water Resources Research*, *48*(3), W03529. https://doi.org/10.1029/2011WR011470

Ebel, B. A., Rengers, F. K., & Tucker, G. E. (2016). Observed and simulated hydrologic response for a first-order catchment during extreme rainfall 3 years after wildfire disturbance. *Water Resources Research*, *52*(12), 9367–9389. https://doi.org/10.1002/2016WR019110

Goutaland, D., Winiarski, T., Dubé, J.-S., Bièvre, G., Buoncristiani, J.-F., Chouteau, M., & Giroux, B. (2008). Hydrostratigraphic characterization of glaciofluvial deposits underlying an infiltration basin using ground penetrating radar. *Vadose Zone Journal*, *7*(1), 194. https://doi.org/10.2136/vzj2007.0003

Goutaland, D., Winiarski, T., Lassabatere, L., Dubé, J. S., & Angulo-Jaramillo, R. (2013). Sedimentary and hydraulic characterization of a heterogeneous glaciofluvial deposit: Application to the modeling of unsaturated flow. *Engineering Geology*, *166*, 127–139. https://doi.org/10.1016/j.enggeo.2013.09.006

Hewelke, E., Szatyłowicz, J., Hewelke, P., Gnatowski, T., & Aghalarov, R. (2018). The impact of diesel oil pollution on the hydrophobicity and CO2 efflux of forest soils. *Water, Air, & Soil Pollution*, *229*(2), 51. https://doi.org/10.1007/s11270-018-3720-6

Imeson, A. C., Verstraten, J. M., van Mulligen, E. J., & Sevink, J. (1992). The effects of fire and water repellency on infiltration and runoff under Mediterranean type forest. *Catena*, *19*(3–4), 345–361. https://doi.org/10.1016/0341-8162(92)90008-Y

Lassabatere, L., Angulo-Jaramillo, R., Goutaland, D., Letellier, L., Gaudet, J. P., Winiarski, T., & Delolme, C. (2010). Effect of the settlement of sediments on water infiltration in two urban infiltration basins. *Geoderma*, *156*(3–4), 316–325. https://doi.org/10.1016/j.geoderma.2010.02.031

Lichner, L., Felde, V. J. M. N. L., Büdel, B., Leue, M., Gerke, H. H., Ellerbrock, R. H., et al. (2018). Effect of vegetation and its succession on water repellency in sandy soils. *Ecohydrology*, *11*(6), e1991. https://doi.org/10.1002/eco.1991

Li, Y., Ren, X., Hill, R., Malone, R., & Zhao, Y. (2018). Characteristics of water infiltration in layered water-repellent soils. *Pedosphere*, *28*(5), 775–792. https://doi.org/10.1016/S1002-0160(17)60414-4

Mansell, R. S. (1970). Infiltration of water into soil columns which have a water-repellent layer. *The Soil and Crop Science Society of Florida Proceedings*.

McGuire, L. A., Rengers, F. K., Kean, J. W., Staley, D. M., & Mirus, B. B. (2018). Incorporating spatially heterogeneous infiltration capacity into hydrologic models with applications for simulating post-wildfire debris flow initiation. *Hydrological Processes*, *32*(9), 1173–1187. https://doi.org/10.1002/hyp.11458

Moody, J. A., Martin, R. G., & Ebel, B. A. (2019). Sources of inherent infiltration variability in postwildfire soils. *Hydrological Processes*, *33*(23), 3010–3029. https://doi.org/10.1002/hyp.13543

Philip, J.-R. (1957). The infiltration equation and its solution. *Soil Science*, *83*(5), 345–357. https://doi.org/10.1097/00010694-195705000-00002

Philip, J.-R. (1969). Theory of infiltration. *Advances in Hydroscience*, *5*, 215–296. https://doi.org/10.1016/B978-1-4831-9936-8.50010-6

Rengers, F. K., McGuire, L. A., Kean, J. W., Staley, D. M., & Youberg, A. M. (2019). Progress in simplifying hydrologic model parameterization for broad applications to post-wildfire flooding and debris-flow hazards. *Earth Surface Processes and Landforms*, *44*(15), 3078–3092. https://doi.org/10.1002/esp.4697

Robichaud, P. R. (2000). Fire effects on infiltration rates after prescribed fire in Northern Rocky Mountain forests, USA. *Journal of Hydrology*, *231*, 220–229. https://doi.org/10.1016/S0022-1694(00)00196-7

Roy, J. L., & McGill, W. B. (2000). Investigation into mechanisms leading to the development, spread and persistence of soil water repellency following contamination by crude oil. *Canadian Journal of Soil Science*, *80*(4), 595–606. https://doi.org/10.4141/S99-091

Rye, C. F., & Smettem, K. R. J. (2017). The effect of water repellent soil surface layers on preferential flow and bare soil evaporation. *Geoderma*, *289*, 142–149. https://doi.org/10.1016/j.geoderma.2016.11.032

Stavi, I., & Rosenzweig, R. (2020). Tillage effect on hydrophobicity and hydrological properties of oil-contaminated sediments in a hyper-arid region. *Arid Land Research and Management*, *34*(1), 26–35. https://doi.org/10.1080/15324982.2019.1599468

Stewart, R. D., & Abou Najm, M. R. (2018a). A comprehensive model for single ring infiltration I: Initial water content and soil hydraulic properties. *Soil Science Society of America Journal*, *82*(3), 548–557. https://doi.org/10.2136/sssaj2017.09.0313

Stewart, R. D., & Abou Najm, M. R. (2018b). A Comprehensive model for single ring infiltration II: Estimating field-saturated hydraulic conductivity. *Soil Science Society of America Journal*, *82*(3), 558–567. https://doi.org/10.2136/sssaj2017.09.0314

Tillman, R. W., Scotter, D. R., Wallis, M. G., & Clothier, B. E. (1989). Water repellency and its measurement by using intrinsic sorptivity. *Soil Research*, *27*(4), 637–644. https://doi.org/10.1071/sr9890637

Vandervaere, J. P., Vauclin, M., & Elrick, D. E. (2000a). Transient flow from tension infiltrometers: I. The two-parameter equation. *Soil Science Society of America Journal*, *64*(4), 1263–1272. https://doi.org/10.2136/sssaj2000.6441263x

Vandervaere, J. P., Vauclin, M., & Elrick, D. E. (2000b). Transient flow from tension infiltrometers: II. Four methods to determine sorptivity and conductivity. *Soil Science Society of America Journal*, *64*(4), 1272–1284. https://doi.org/10.2136/sssaj2000.6441272x

Winiarski, T., Bedell, J.-P., Delolme, C., & Perrodin, Y. (2006). The impact of stormwater on a soil profile in an infiltration basin. *Hydrogeology Journal*, *14*(7), 1244–1251. https://doi.org/10.1007/s10040-006-0073-9

Winitzki, S. (2003). Uniform Approximations for Transcendental Functions. In V. Kumar, M. L. Gavrilova, C. J. K. Tan, & P. L'Ecuyer (Eds.), *Computational Science and Its Applications — ICCSA 2003. ICCSA 2003, Lecture Notes in Computer Science* (Vol. 2667). Berlin, Heidelberg: Springer. https://doi.org/10.1007/3-540-44839-X_82